THE OXIDATION OF METHANOL ON A SILVER (110) CATALYST

Israel E. WACHS * and Robert J. MADIX

Department of Chemical Engineering, Stanford University, Stanford, California 94305, USA

The oxidation of methanol was studied on a Ag(110) single-crystal by temperature programmed reaction spectroscopy. The Ag(110) surface was preoxidized with oxygen-18, and deuterated methanol, CH_3OD, was used to distinguish the hydroxyl hydrogen from the methyl hydrogens. Very little methanol chemisorbed on the oxygen-free Ag(110) surface, and the ability of the silver surface to dissociatively chemisorb methanol was greatly enhanced by surface oxygen. CH_3OD was selectively oxidized upon adsorption at 180 K to adsorbed CH_3O and $D_2{}^{18}O$, and at high coverages the $D_2{}^{18}O$ was displaced from the Ag(110) surface. The methoxide species was the most abundant surface intermediate and decomposed via reaction channels at 250, 300 and 340 K to H_2CO and hydrogen. Adsorbed H_2CO also reacted with adsorbed CH_3O to form H_2COOCH_3 which subsequently yielded $HCOOCH_3$ and hydrogen. The first-order rate constant for the dehydrogenation of D_2COOCH_3 to $DCOOCH_3$ and deuterium was found to be $(2.4 \pm 2.0) \times 10^{11} \exp(-14.0 \pm 0.5 \text{ kcal/mole} \cdot RT)\sec^{-1}$. This reaction is analogous to alkoxide transfer from metal alkoxides to aldehydes in the liquid phase. Excess surface oxygen atoms on the silver substrate resulted in the further oxidation of adsorbed H_2CO to carbon dioxide and water. The oxidation of methanol on Ag(110) is compared to the previous study on Cu(110).
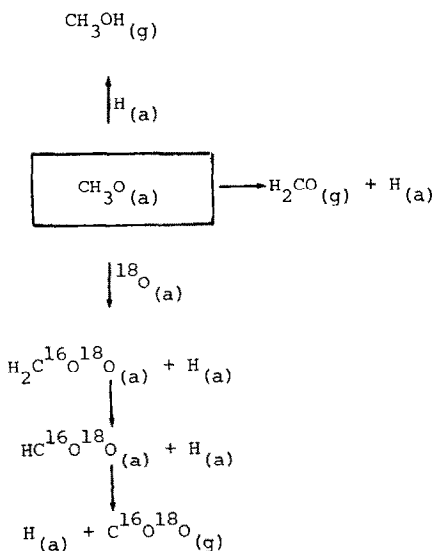
1. Introduction

The classical process for the manufacture of formaldehyde by the oxidation of methanol employs silver or copper catalysts in the form of gauze or pellets at approximately 600 and 725°C, respectively [1]. The characteristics of silver and copper catalysts for the oxidation of methanol were compared during the early development of this process and the silver catalysts were found to be slightly more selective toward the formation of formaldehyde [2]. As a result of these investigations silver has almost completely replaced copper as the catalyst in the commercial processes operating in the classical mode [3]. An alternate and more modern process for manufacturing formaldehyde employs an oxide catalyst near 350°C, such as iron—molybdenum oxide [4]. All of these processes are still currently used for the commercial oxidation of methanol to formaldehyde. The purpose of this study was to determine the mechanism and kinetics of the oxidation of methanol to formaldehyde on silver with the modern tools of surface science and compare the

---

* Present address: Corporate Research Laboratories, Exxon Research and Engineering Company, Linden, New Jersey 07036, USA.

results with the previous investigation on copper [5]. For the sake of comparison the results on copper will be briefly summarized.

The oxidation of methanol was investigated on a copper (110) single crystal surface by the method of temperature programmed reaction spectroscopy (TPRS) [5]. The Cu(110) surface was preoxidized with $^{18}O_2$, and deuterated methanol, CH_3OD, was used to distinguish the hydroxyl hydrogen from the methyl hydrogens. Very little methanol chemisorbed on the oxygen-free Cu(110) surface, and the ability of the copper surface to dissociatively adsorb methanol was greatly enhanced by the presence of preadsorbed oxygen. It was concluded that during adsorption methanol interacted with surface oxygen-18 through its hydroxyl hydrogen to form $CH_3O_{(a)}$ and $D_2{}^{18}O$. The different reaction pathways available to surface methoxide, $CH_3O_{(a)}$, on Cu(110) are schematically presented in scheme 1.

Scheme 1.

$$CH_3OH_{(g)}$$

$$\uparrow H_{(a)}$$

$$\boxed{CH_3O_{(a)}} \longrightarrow H_2CO_{(g)} + H_{(a)}$$

$$\downarrow {}^{18}O_{(a)}$$

$$H_2C{}^{16}O{}^{18}O_{(a)} + H_{(a)}$$

$$\downarrow$$

$$HC{}^{16}O{}^{18}O_{(a)} + H_{(a)}$$

$$\downarrow$$

$$H_{(a)} + C{}^{16}O{}^{18}O_{(g)}$$

The hydrogen atoms released in the various reaction steps either recombined to form H_2, reduced $^{18}O_{(a)}$ to $H_2{}^{18}O$, or reacted with surface methoxide to form methanol. The methoxide was the most abundant surface intermediate and $D_2{}^{18}O$ accounted for approximately 75% of the water produced. To a lesser extent some methanol was oxidized to surface formate which subsequently decomposed to $C^{16}O^{18}O$ and hydrogen. The experimental results showed that the selectivity of the oxidation of CH_3OD on Cu(110) was 80% H_2CO and 20% $C^{16}O^{18}O$, and compared well with the H_2CO selectivity of 80–90% observed industrially [3]. The above mechanism showed that H_2CO resulted from the dehydrogenation of the methoxide intermediate. As is shown below the oxidation of methanol on Cu(110) and Ag(110) surface exhibited many similarities, but striking differences were also observed.

2. Experimental

The oxidation of CH_3OD on Ag(110) was studied by TPRS in the stainless steel ultrahigh vacuum system previously described [6]. The UHV chamber was equipped with a PHI four-grid LEED—Auger optics, an argon ion bombardment gun and a UTI-100C quadrupole mass spectrometer. The Ag(110) sample could be cooled to about 180 K by heat conduction through a copper braid attached to a liquid nitrogen cooled copper finger. The sample was heated from the rear by radiation from a tungsten filament; a heating rate of about 15 K sec^{-1} was employed. Deuterated methanol, CH_3OD (99 atom% D), obtained from ICN Life Sciences was introduced onto the front face of the silver crystal through a stainless steel dosing syringe backed by the methanol vapor pressure obtained above liquid CH_3OD at $-84°C$. The methanol was purified as previously described [5]. The mass spectrometer signal for each product produced during the flash desorption was directly proportional to the desorption rate because of the high pumping speed of the system. Peak temperatures were reproducible to within ±5 K from day to day.

The Ag(110) sample was cut from a crystal having 5N purity and was not etched prior to mounting in the UHV system. The initial Auger spectrum showed large sulfur and carbon peaks and trace amounts of tellurium. The sulfur and carbon peaks disappeared after the first argon bombardment cycle but small Te peaks were still present. The Te peaks were not observed following many cycles of argon bombardment and annealing to 800 K for several minutes. The Auger spectrum of the clean (110) oriented silver single crystal is presented in fig. 1, and the major silver peaks are labeled. The same Auger spectrum was obtained for the Ag(110) surface by other investigators [7,8]. The small Auger peaks observed at about 125, 150 and
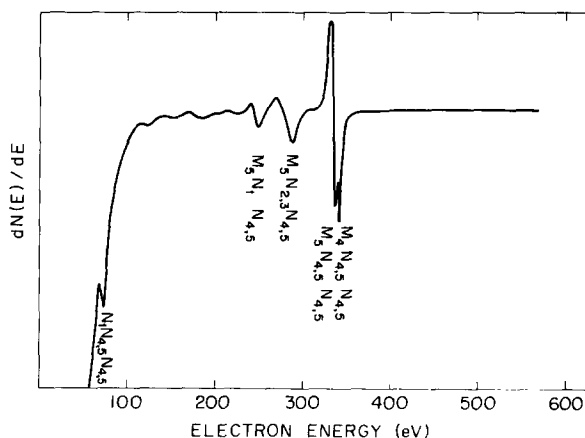

Fig. 1. AES spectrum of the clean Ag(110) surface.

183 eV were also reported in previous studies and are possibly a combination of trace amounts of molybdenum [9] and other silver transitions [10]. The presence of small quantities of carbon was not readily observable because of overlap with the silver M_5 transitions, and the absence of surface carbon was deduced from the ratio of $M_5N_1N_{4,5}$ and $M_5'N_{2,3}N_{4,5}$ silver peaks [7]. After successive cycles of argon bombardment this ratio was between 0.45 and 0.50 depending on the modulation voltage (usually between 5 and 6 V peak to peak), and this value was defined as a carbon-free Ag(110) surface.

The sharp LEED pattern of the clean Ag(110) single crystal indicated that the surface was highly ordered. The LEED patterns subsequent to the adsorption of oxygen on the Ag(110) were only briefly examined and were found to agree with those previously reported for this system [7]. At low exposures of oxygen the formation of streaks along the (001) direction in the diffraction pattern were observed; these streaks have been attributed by Bradshw et al. to oxygen atoms adsorbed in the troughs of the (110) surface [7]. The LEED patterns corresponding to high oxygen coverages on Ag(110) were not examined in the present study in order to avoid adverse effects on the Vacion pump and the generation of ambient carbon dioxide and carbon monoxide in the vacuum chamber resulting from the high oxygen exposures needed.

The total amount of oxygen adsorbed on the Ag(110) surface for a given oxygen exposure at room temperature was measured by flashing the sample to 650 K, since oxygen desorbed from the silver surface at about 575 K. The flash desorption spectrum of $^{18}O_2$ observed [11] exhibited the same behavior as a function of oxygen coverage as previously reported in the literature [7]. The amount of oxygen adsorbed on the Ag(110) surface for a given background exposure of oxygen was increased by a factor of 3–4 by switching on the ionizer of the mass spectrometer and facing the front side of the crystal toward the ionizer. The relative amounts of oxygen adsorbed with the mass spectrometer filament on and off is shown in fig. 2 as a function of oxygen exposure based on the $^{18}O_2$ pressure in the chamber (1 Langmuir is defined as 1×10^{-6} Torr sec of exposure). The initial sticking probability of oxygen on the Ag(110) surface was previously estimated to be about 10^{-3} by Bradshaw et al. [7]; the surface coverages of oxygen were calculated from knowledge of this parameter. Since the M.S. off curve was linear at low exposures of oxygen, indicating a constant sticking probability, the surface coverages of oxygen with the M.S. off were determined from fig. 2. These results were then corrected for the oxygen coverages on Ag(110) obtained with the M.S. on and are presented in table 1. These values are, at best, only reliable to within a factor of two due to the uncertainty in the initial sticking probability of oxygen on the Ag(110) surface.

Typically the Ag(110) sample was oxidized with enriched oxygen (99% $^{18}O_2$) introduced into the background of the UHV chamber through a variable leak valve. The mass spectrometer was always on during the adsorption process and the front face of the sample faced the mass spectrometer; this procedure assured that oxygen was selectively adsorbed on the *front face* of the Ag(110) surface. An oxygen back-
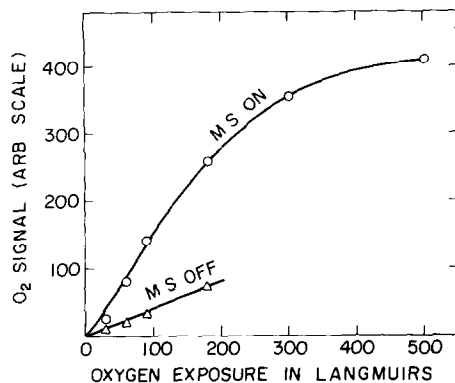
Fig. 2. The relative amounts of oxygen adsorbed on the Ag(110) surface with the mass spectrometer on and off as a function of oxygen exposure. The Ag(110) sample was maintained at 295 ± 10 K when exposed to $10^{-7}-10^{-6}$ Torr of oxygen.

ground pressure of $10^{-7}-10^{-6}$ Torr was maintained throughout the adsorption of oxygen and the silver sample was kept at 295 ± 10 K. The crystal was then cooled to about 180 K and CH_3OD was adsorbed on the partially oxidized surface. The sample was then flashed, and the various products were monitored with the mass spectrometer. Blank flash desorption experiments without the adsorption of CH_3OD verified that over the range of oxygen exposures studied, 0–180 L with the M.S. on, background carbon dioxide and carbon monoxide did not coadsorb on the Ag(110) surface.

The products observed in this study were identified by carefully comparing their observed cracking patterns in the mass spectrometer with those tabulated in the literature and those obtained in the present UHV chamber. Once the product was identified, the ionized parent molecule. i.e. $m/e = 33$ for CH_3OD, $m/e = 30$ for H_2CO, etc., was used to monitor the product. The only exception was CH_3OH for

Table 1
The surface coverages of oxygen on Ag(110) with the M.S. on; the surface concentrations of oxygen are based on an initial sticking probability of about 10^{-3} with the M.S. off [7]

Oxygen exposure with M.S. on (L)	Surface coverage of oxygen (fraction of monolayer)
30	0.06
60	0.19
90	0.34
180	0.61
300	0.85
500	0.99

which $m/e = 31$ was monitored in order to minimize overlap with other product signals, but even the $m/e = 31$ signal always included cracking contributions from HCOOCH$_3$. A more extensive discussion on product identification by mass spectrometry will be found in the Appendix.

3. Results

A variety of reaction products resulted from the adsorption of CH$_3$OD at ~180 K to saturation on a Ag(110) surface predosed with 60 L oxygen-18 (M.S. on) as shown in fig. 3. The first species to leave the surface *during* the flash desorption was CH$_3$OD. Subsequently H$_2$CO, HCOOCH$_3$, CH$_3$OH and H$_2$ desorbed simultaneously near 250 K from the Ag(110) surface indicating that they shared a common rate-limiting step. These products were evolved in a reaction-limited step, since otherwise they would have desorbed at the lower surface temperatures characteristic of their desorption spectra (see table 2). CH$_3$OH was produced as a reaction product even though CH$_3$OD was initially adsorbed on the silver surface. The deuterium atom was selectively removed from CH$_3$OD upon adsorption, because D$_2$^{18}O was the first product to desorb and was *displaced from the Ag(110) surface during the adsorption process*. Trace amounts of HD^{18}O and H$_2$^{18}O were also observed, but D$_2$^{18}O accounted for more than 90% of the water formed.

The evolution of D$_2$^{18}O *during the flash* is shown in fig. 4. The D$_2$^{18}O peak temperatures shifted to lower temperatures with increasing methanol exposure, but at high exposures almost no D$_2$^{18}O was observed during the flash; the D$_2$^{18}O signal

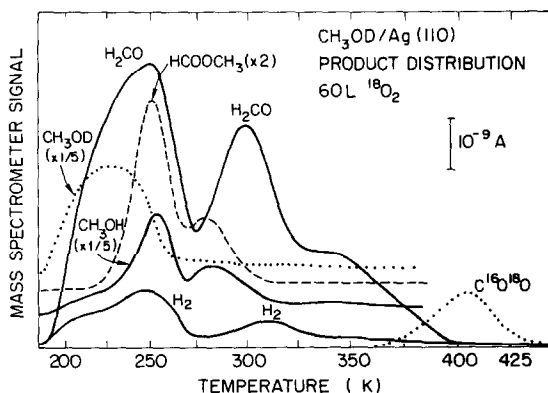Fig. 3. The thermal programmed reaction spectrum obtained following CH$_3$OD adsorption at 180 K on a Ag(110) surface on which oxygen-18 was preadsorbed at 295 ± 10 K. The ^{18}O$_2$ exposure applied was 60 L with the M.S. on; the CH$_3$OD exposure was 150 sec. These curves are uncorrected for detection sensitivities and the CH$_3$OH spectrum contains cracking contributions from HCOOCH$_3$.

Table 2

Characteristic desorption parameters for several molecules from the oxygen-free Ag(110) surface. Adsorption was always performed with the Ag(110) sample cooled to 180 K; E^* is the activation energy calculated for a single first-order rate-limiting step from the peak temperatures, T_p, assuming the pre-exponential factor to be 10^{13} sec^{-1}

Molecule	T_p (K)	E^* (kcal/mole)	Source
D_2/D_{atoms}	228	13.3	This work
H_2CO/H_2CO	228	13.3	This work
$HCOOCH_3/HCOOCH_3$	235	13.7	This work

exhibited a maximum with CH_3OD exposure. Since the $D_2{}^{18}O$ substrate bond appeared to be weakened with increasing total coverage, the diminished $D_2{}^{18}O$ signal at high coverage suggested that $D_2{}^{18}O$ was displaced by other intermediates from the Ag(110) surface.

The $D_2{}^{18}O$ signal was thus monitored *during the adsorption of CH_3OD at 180 K* on the partially oxidized Ag(110) substrate. The front face of the (110) oriented silver crystal was preferentially oxidized by dissociating the oxygen in the mass spectrometer. As a blank calibration, the backside of the Ag(110) sample was exposed to CH_3OD from the doser, and almost no $D_2{}^{18}O$ formed. When the sample
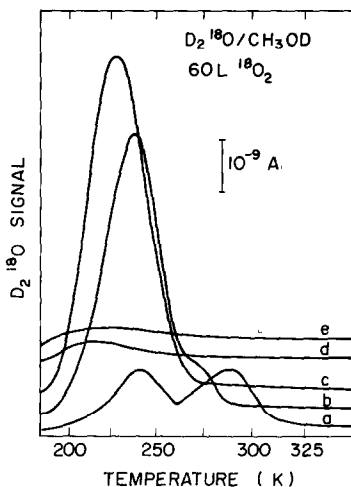

Fig. 4. The $D_2{}^{18}O$ desorption spectra subsequent to the oxidation of CH_3OD on Ag(110). The CH_3OD was adsorbed at 180 K on a Ag(110) surface that was predosed with $^{18}O_2$ at 295 ± 10 K. The oxygen exposure applied was 60 L with the M.S. on. The CH_3OD exposures were (a) 5 sec, (b) 13 sec, (c) 25 sec, (d) 50 sec and (e) 75 sec.

was rotated to expose the oxidized face of the Ag(110) crystal, a large $D_2^{18}O$ signal was observed. The $D_2^{18}O$ signal initially increased as a function of time, and then decayed towards zero when almost all the ^{18}O atoms on the Ag(110) surface were consumed. The HD ^{18}O and $H_2^{18}O$ signals were also monitored in the same manner, but only trace amounts were formed. This experiment verified that $D_2^{18}O$ was selectively formed and displaced from the partially oxidized Ag(110) surface by other species during the adsorption of CH_3OD at 180 K.

Subsequent to *low exposures* of CH_3OD (less than 25 sec) some $H_2^{18}O$ and HD ^{18}O were formed *during* the flash because not all of the surface oxygen-18 atoms were consumed during adsorption at 180 K by reaction to form $D_2^{18}O$. The absence of the products $H_2^{18}O$ and HD ^{18}O for methanol exposures greater than 25 sec was not due to displacement from the silver surface, since substantial $H_2^{18}O$ and HD ^{18}O signals were not detected during adsorption at 180 K, but was the result of the selective titration of ^{18}O by CH_3OD to form $D_2^{18}O$ upon adsorption. The HD ^{18}O peak temperatures exhibited approximately the same behavior as shown in fig. 4 for $D_2^{18}O$ as a function of methanol exposure, but the HD ^{18}O peak temperatures were about 5−10 K higher. The HD ^{18}O produced on the unsaturated surfaces resulted from the reaction of ^{18}OD, formed during adsorption of CH_3OD at 180 K, and hydrogen atoms released by surface intermediates during the early stages of the flash (see fig. 3). The $H_2^{18}O/CH_3OD$ peaks formed at low exposures coincided with the H_2/CH_3OD peaks. The $H_2^{18}O$ peaks were observed at low surface coverages opf methanol because excess oxygen was present on the surface, and some of the reaction products were further oxidized before desorbing from the Ag(110) surface. These results revealed that the ^{18}O atoms on the Ag(110) surface could be selectively reacted or *titrated* to $D_2^{18}O$ by exposing the partially oxidized silver surface to high exposures of CH_3OD at 180 K.

No HD or D_2 was observed to desorb throughout the entire temperature range, indicating that *all of the deuterium atoms released upon adsorption resulted in the formation of water*. This result suggested that CH_3OH was produced from CH_3OD that had released its D atom upon adsorption to form $CH_3O_{(a)}$ which subsequently reacted with a surface H atom to form CH_3OH. CH_3OH was again evolved with $HCOOCH_3$ at about 280 K and to a minor extent at about 300 and 340 K with H_2CO and H_2 (see figs. 3 and 10). The CH_3OH peaks at 300 and 340 K are not well defined in fig. 3, but were distinct at higher detection sensitivities. The simultaneous desorption of H_2, H_2CO and CH_3OH at about 300 and 340 K revealed that these products also originated from the decomposition of a common surface intermediate since the *desorption* states for these molecules appeared at lower surface temperatures. The final products to desorb during the flash were $C^{16}O^{18}O$ and $H_2(\gamma)/CH_3OD$ (very small signal) at 402 K which resulted from the decomposition of a formate intermediate, as discussed below. No other products were observed; in particular, carbon monoxide, methane, methylal, dimethyl ether and ethanol were absent.

The results observed for the oxidation of CH_3OD on the silver (110) surface are

Table 3
Summary of the results observed for the oxidation of CH_3OD on $Ag(110)$; the $Ag(110)$ surface was oxidized at 295 ± 10 K and exposed to 150 s of CH_3OD at 180 K

State	T_p (K)	E (kcal/mole)	ν (sec^{-1})	E^* [a] (kcal/mole)
$HCOOCH_3(\alpha_1)/CH_3OD$	250	13.1 ± 0.6 [b]	$(4.5 \pm 3.5) \times 10^{11}$ [b]	14.6
$HCOOCH_3(\alpha_2)/CH_3OD$	280 ± 3	13.3 ± 0.4 [c]	$(2.5 \pm 1.5) \times 10^{10}$ [c]	16.3
$CH_3OH(\alpha_1)/CH_3OD$	252	–	–	14.7
$CH_3OH(\alpha_2)/CH_3OD$	280 ± 3	–	–	16.3
$CH_3OH(\beta_2)/CH_3OD$	300	–	–	17.6
$CH_3OH(\beta_3)/CH_3OD$	340	–	–	20.0
$H_2CO(\beta_1)/CH_3OD$	250	–	–	14.6
$H_2CO(\beta_2)/CH_3OD$	300	–	–	17.6
$H_2CO(\beta_3)/CH_3OD$	340 ± 10	–	–	20.0
$H_2(\beta_1)/CH_3OD$	250	–	–	14.6
$H_2(\beta_2)/CH_3OD$	312	–	–	18.3
$H_2(\beta_3)/CH_3OD$	350	–	–	20.6
$H_2(\gamma)/CH_3OD$	402	–	–	23.8
$C^{16}O^{18}O/CH_3OD$	402	22.2 ± 0.5 [b]	$(1.1 \pm 0.7) \times 10^{12}$ [b]	23.8
$DCOOCH_3/CH_3OD, D_2CO$	273	14.0 ± 0.5 [b]	$(2.4 \pm 2.0) \times 10^{11}$ [b]	16.0

[a] E^* is the activation energy calculated for a single first-order rate-limiting step from T_p assuming $\log_{10} \nu = 13$.
[b] The kinetic parameters were calculated by plotting $\ln(R/C)$ versus $1/T$ [12].
[c] The kinetic parameters were calculated from isothermal plots [12].

tabulated in table 3. The previous results obtained for the oxidation of CH_3OH on Copper (110) [5] are presented in table 4 for comparison. All of the reactions listed exhibited *first-order* kinetics as evidenced by the independence of peak temperature on the initial amount of reactant adsorbed.

The mechanism of the formation of all reaction products subsequent to high exposures of CH_3OD on partially oxidized $Ag(110)$, except methyl formate, thus appears to be similar to that observed for methanol oxidation on copper. CH_3OD dissociatively adsorbed on both partially oxidized substrates to yield adsorbed CH_3O and $D_2^{18}O$, and the different reaction products resulted from the surface chemistry of the methoxide intermediate. Several reaction pathways were available to the surface methoxide since it could, as discussed in the introduction, (1) dehydrogenate to formaldehyde and hydrogen; (2) be reduced by surface hydrogen atoms to CH_3OH; and (3) be oxidized to $HC^{16}O^{18}O$. The mechanism of $HCOOH_3$ formation will now be addressed.

Several methyl formate spectra are shown in fig 5 as a function of CH_3OD exposure. Two $HCOOCH_3$ peaks (α_1 and α_2) were present on the $Ag(110)$ surface. The $HCOOCH_3(\alpha_1)/CH_3OD$ state was dominant at higher exposures. The invariance of

Table 4
Summary of the results observed for the oxidation of CH_3OH on $Cu(110)$; the $Cu(110)$ surface was oxidized at 295 ± 10 K and exposed to CH_3OH at 180 K; the heating rate was $4-5$ K s^{-1}

State	T_p (K)	E (kcal/mole)	ν (sec^{-1})	E^* [a] (kcal/mole)
$CH_3OH(\alpha_1)/CH_3OH$	200 ± 5	—	—	12.1
$CH_3OH(\alpha_2)/CH_3OH$	245 ± 5	—	—	14.8
$CH_3OH(\alpha_3)/CH_3OH$	275	—	—	16.7
$CH_3OH(\beta_1)/CH_3OH$	330 ± 5	—	—	20.1
$CH_3OH(\beta_2)/CH_3OH$	365	—	—	22.4
$CH_3OH(\beta_3)/CH_3OH$	390	—	—	23.9
$H_2CO(\beta_2)/CH_3OH$	365	22.1 ± 0.1 [c]	$(5.2 \pm 1.6) \times 10^{12}$ [c]	22.4
$H_2CO(\beta_3)/CH_3OH$	392	19.3 ± 0.4 [b]	$(1.5 \pm 0.7) \times 10^{10}$ [b]	24.0
$H_2(\beta_1)/CH_3OH$	325 ± 5	—	—	19.8
$H_2(\beta_2)/CH_3OH$	370	22.0 [c]	3.6×10^{12} [c]	22.6
$H_2(\beta_3)/CH_3OH$	390	—	—	23.9
$H_2(\gamma)/CH_3OH$	470	30.9 ± 0.2 [c]	$(8.0 \pm 2.0) \times 10^{13}$ [c]	29.0
$C^{16}O^{18}O/CH_3OH$	470	30.9 ± 0.2 [c]	$(8.0 \pm 2.0) \times 10^{13}$ [c]	29.0
$H_2^{18}O(\delta_1)/CH_3OH$	238	—	—	14.3
$H_2^{18}O(\delta_2)/CH_3OH$	290	—	—	17.6
$H_2^{18}O(\delta_3)/CH_3OH$	320	—	—	19.5
$H_2^{18}O(\gamma)/CH_3OH$	470	30.9 ± 0.2 [c]	$(8.0 \pm 2.0) \times 10^{13}$ [c]	29.0

[a] E^* is the activation energy calculated for a single first-order rate-limiting step from T_p assuming $\log_{10} \nu = 13$.

[b] The kinetic parameters were calculated by plotting $\ln(R/C)$ versus $1/T$ [12].

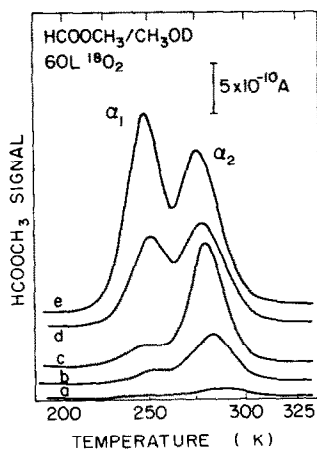[c] The kinetic parameters were calculated by the method of heating rate variation [12].

Fig. 5. The formation of $HCOOCH_3$ from the oxidation of CH_3OD on a Ag(110) surface. The Ag(110) sample was oxidized by 60 L $^{18}O_2$ with the M.S. on at 295 ± 10 K, and CH_3OD was adsorbed on the partially oxidized surface at 180 K. The CH_3OD exposures were (a) 5.0 sec, (b) 13.0 sec, (c) 19.0 sec, (d) 25 sec and (e) 75 sec.

the HCOOCH$_3$ α_1 and α_2 peak temperatures with coverage indicated that the production of methyl formate was limited by a first-order surface reaction, since methyl formate was shown to desorb with a peak temperature of approximately 235 K from the Ag(110) substrate (see table 2). The first-order rate constants for the production of methyl formate were determined to be:

$k_{HCOOCH_3(\alpha_1)/CH_3OD}$

$$= (4.5 \pm 3.5) \times 10^{11} \exp(-13.1 \pm 0.6 \text{ kcal/mole} \cdot RT) \sec^{-1} , \tag{1}$$

$k_{HCOOCH_3(\alpha_2)/CH_3OD}$

$$= (2.5 \pm 1.5) \times 10^{10} \exp(-13.3 \pm 0.4 \text{ kcal/mole} \cdot RT) \sec^{-1} . \tag{2}$$

It was not clear to what extent these kinetic parameters for the formation of HCOOCH$_3(\alpha_1)$/CH$_3$OD were influenced by the sequential desorption step for methyl formate because the peak temperature was not much greater than the HCOOCH$_3$/HCOOCH$_3$ desorption peak temperature itself.

Methyl formate,

$$\begin{array}{c} O \\ \| \\ DCOCH_3 \end{array} ,$$
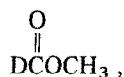
was also found to be a major reaction product following coadsorption of D$_2$CO and CH$_3$OD on the partially oxidized Ag(110) surface at 180 K. The DCOOCH$_3$ spectra are shown in fig. 6 as a function of D$_2$CO and CH$_3$OD exposure (D$_2$CO and CH$_3$OD were premixed in the dosing line in approximately equal amounts before dosing). The DCOOCH$_3$ peak temperature was constant for the different coverages investi-

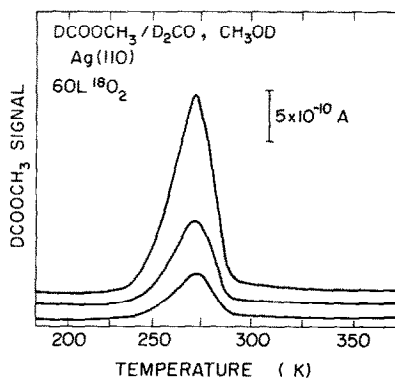Fig. 6. DCOOCH$_3$ desorption subsequent to the coadsorption of D$_2$CO and CH$_3$OD at 180 K on a partially oxidized Ag(110) surface. The Ag(110) surface was oxidized by 60 L ^{18}O$_2$ with the M.S. on at 295 $\pm$ 10 K. The exposures of the D$_2$CO and CH$_3$OD mixture were (a) 5 sec, (b) 13 sec, and (c) 25 sec.

gated, and $DCOOCH_3$ formation from D_2CO and CH_3OD was therefore also limited by a first-order surface reaction. In addition, D_2 and CH_3OD also desorbed from the $Ag(110)$ surface at the same temperature as $DCOOCH_3$. Since the CH_3OD deuterium atom was oxidized to $D_2{}^{18}O$ upon adsorption, this experiment revealed that methyl formate was produced from the decomposition of a surface complex that resulted from the interaction of formaldehyde (D_2CO) and CH_3O. The surface complex and the reaction steps responsible for methyl formate and the other products were

$$D_2COOCH_{3(a)} \rightarrow D_{(a)} + DCOOCH_{3(g)} \,, \tag{3}$$

$$D_{(a)} + D_{(a)} \rightarrow D_{2(g)} \,, \tag{4}$$

$$D_{(a)} + CH_3O_{(a)} \rightarrow CH_3OD_{(g)} \,. \tag{5}$$

Since the formation of these products occurred via a first-order surface process, reaction step (3) was rate-limiting.

The first-order rate constant for the formation of $DCOOCH_3$, step (3), was determined by plotting the natural logarithm of the rate divided by the coverage versus inverse surface temperature [12] for the series of curves presented in fig. 6 as shown in fig. 7. The kinetic parameters were found to be

$$k_{DCOOCH_3/D_2CO,CH_3OD}$$

$$= (2.4 \pm 2.0) \times 10^{11} \exp(-14.0 \pm 0.5 \text{ kcal/mole} \cdot RT) \sec^{-1} \,. \tag{6}$$

This rate constant is very similar to the first-order rate constants for $HCOOCH_3(\alpha_1)/$
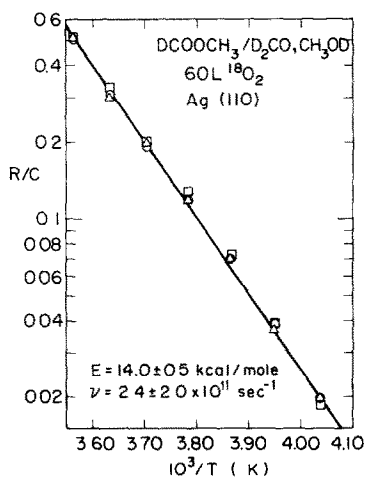

Fig. 7. The first-order rate constant for the formation of $DCOOCH_3$ following the coadsorption of D_2CO and CH_3OD on the partially oxidized $Ag(110)$ surface. The kinetic parameters were calculated from the data of fig. 6.

CH_3OD and $HCOOCH_3(\alpha_2)/CH_3OD$ and suggests that the same surface complex was responsible for methyl formate formation in the oxidation of CH_3OD on Ag(110).

The differences in the peak positions observed for $HCOOCH_3/CH_3OD$ (250 and 280 ± 3 K) and $DCOOCH_3/D_2CO$, CH_3OD (273 K) were the result of isotope effects related to breaking the H–C bond in the formation of $HCOOCH_3$ from H_2COOCH_3 and a D–C bond in the formation of $DCOOCH_3$ from D_2COOCH_3, as was verified by forming the various deuterated isotopes of methyl formate on the partially oxidized Ag(110) surface from a 50 : 50 mixture of CH_3OD and CD_3OD at 180 K. The adsorption of such a mixture on the partially oxidized silver surface resulted in the formation of $CH_3O_{(a)}$, $CD_3O_{(a)}$, $H_2CO_{(a)}$, and $D_2CO_{(a)}$ which interacted to produce the different deuterated isotopes of methyl formate. The $DCOOCH_3$ and $DCOOCD_3$ flash curves exhibited only *one peak* at 273 K; the $HCOOCH_3$ and $HCOOCD_3$ flash curves exhibited *two peaks* at 250 and 280 ± 3 K. Although the origin of this behavior is not completely understood, the above experiment demonstrated that it was related to an isotope effect and not a mechanistic difference.

A small quantity of methyl formate, $DCOOCH_3$, was also produced following coadsorption of DCOOH and CH_3OD on the partially oxidized Ag(110) surface; the peak position observed was approximately 420 K. The formation of methyl formate from formic acid and methanol is a well-known organic reaction [13], but on the silver substrate this reaction pathway was not responsible for the formation of methyl formate from methanol below room temperature.

In order to examine the function of oxygen upon the oxidation of methanol on silver, the oxygen exposure was varied from 0–180 L while a constant methanol exposure of 150 sec was maintained. The marked dependence of the various reaction product signals upon the surface concentration of oxygen is shown in fig. 8.
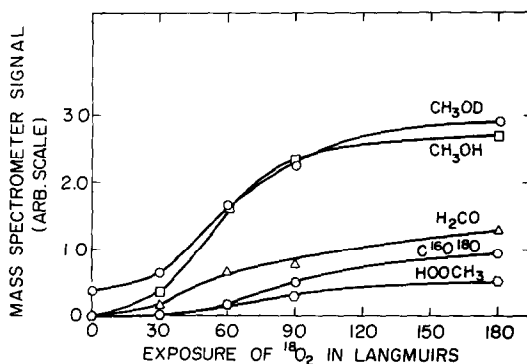

Fig. 8. The influence of oxygen exposure upon the production of the various reaction products following a 150 sec exposure of CH_3OD at 180 K. The Ag(110) surface was always oxidized at 295 ± 10 K with the M.S. on.

Almost no reaction products were observed on the oxygen-free silver surface, but a small amount of undissociated CH_3OD did adsorb on the Ag(110) surface. All of the product signals, including undissociated CH_3OD, exhibited a strong dependence upon the oxygen exposure. These results demonstrated that methanol interacted with surface oxygen atoms during the adsorption process, since surface oxygen enhanced the sticking probability of methanol on silver. The selective formation of $D_2{}^{18}O$ during the adsorption of CH_3OD and the absence of HD and D_2 from the spectrum further suggested that the *hydroxyl end of the methanol molecule interacted with the surface oxygen atom during the adsorption process.*

The amount of undissociated CH_3OD adsorbed on the Ag(110) surface increased substantially with increasing oxygen coverage. The enhanced adsorption was most likely due to the stabilization of CH_3OD on the silver surface through interaction with other surface intermediates, since the oxygen-free silver surface barely adsorbed any CH_3OD. The undissociated CH_3OD did not interact with surface oxygen atoms, since they were displaced by $D_2{}^{18}O$ formation. Thus, the intermediate responsible for stabilization of adsorbed CH_3OD was probably methoxide, since it was the most abundant surface intermediate following methanol adsorption at 180 K, and since CH_3OD desorbed from the silver surface in the temperature range in which the surface methoxide began to dissociate to formaldehyde (see fig. 3).

The binding states of the various surface intermediates on ·Ag(110) were not altered by the different surface concentrations of oxygen examined because the peak temperatures of the various reaction products were constant with oxygen exposure, and no new peaks were observed. This result indicated that over the range of surface oxygen concentration investigated the Ag(110) surface did not reconstruct.

4. Discussion *

The results of this work led to the following conclusions about the oxidation of CH_3OD on Ag(110):

(1) Surface oxygen enhanced both the dissociative and non-dissociative chemisorption of CH_3OD; only a small quantity of undissociated methanol was adsorbed on the oxygen-free Ag(110) surface.

(2) The hydroxyl group of the CH_3OD molecule interacted with surface ^{18}O atoms during the dissociative adsorption process to form adsorbed CH_3O and $D_2{}^{18}O$.

(3) The binding energy of $D_2{}^{18}O$ was weakened by other surface intermediates, and $D_2{}^{18}O$ was eventually displaced from the Ag(110) surface into the gas phase following high exposures of methanol at 180 K.

(4) $HCOOCH_3$ was formed from the dissociation of the surface complex

---

* Further discussion of the product peaks for H_2, CH_3OH, H_2CO, CH_3OD is presented in Appendix I.

H_2COOCH_3 which resulted from the addition of adsorbed CH_3O to adsorbed H_2CO.
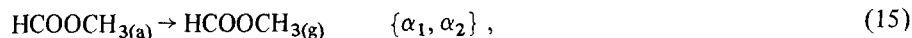
(5) The simultaneous appearance of CH_3OH, H_2CO and H_2 resulted from the reactions of an adsorbed CH_3O intermediate.

(6) $C^{16}O^{18}O$ originated from the decomposition of adsorbed $HC^{16}O^{18}O$. (See below.)

(7) Formaldehyde produced during the flash was further oxidized to $HC^{16}O^{18}O$ and $H_2^{18}O$ by excess surface oxygen when the ratio of the surface concentrations $^{18}O/CH_3O$ was greater than zero.

These observations suggested that following *high* methanol exposures the ratio of the surface species $^{18}O/CH_3O$ approached zero, and the major reaction steps involved in the oxidation of CH_3OD on Ag(110) were * :

$$CH_3OD_{(g)} + {}^{18}O_{(a)} \rightarrow CH_3O_{(a)} + {}^{18}OD_{(a)} \; . \tag{7a}$$

$$CH_3OD_{(g)} + {}^{18}OD_{(a)} \rightarrow CH_3O_{(a)} + D_2^{18}O_{(a)} \; , \tag{7b}$$

$$CH_3OD_{(g)} + CH_3O_{(a)} \rightarrow CH_3OD_{(a)}(+)CH_3O_{(a)} \; , \tag{8}$$

$$D_2^{18}O_{(a)} \rightarrow D_2^{18}O_{(g)} \; , \tag{9}$$

$$CH_3OD_{(a)}(+)CH_3O_{(a)} \rightarrow CH_3OD_{(g)} + CH_3O_{(a)} \; , \tag{10}$$

$$CH_3O_{(a)} \rightarrow H_{(a)} + H_2CO_{(a)} \; , \tag{11}$$

$$H_2CO_{(a)} \rightarrow H_2CO_{(g)} \qquad \{\beta_1\} \; , \tag{12}$$

$$H_2CO_{(a)} + CH_3O_{(a)} \rightarrow H_2COOCH_{3(a)} \; , \tag{13}$$

$$H_2COOCH_{3(a)} \rightarrow HCOOCH_{3(a)} + H_{(a)} \; , \tag{14}$$

$$HCOOCH_{3(a)} \rightarrow HCOOCH_{3(g)} \qquad \{\alpha_1, \alpha_2\} \; , \tag{15}$$

$$H_{(a)} + H_{(a)} \rightarrow H_{2(g)} \qquad \{\beta_1\} \; , \tag{16}$$

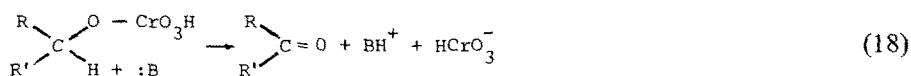$$H_{(a)} + CH_3O_{(a)} \rightarrow CH_3OH_{(g)} \qquad \{\alpha_1, \alpha_2\} \; . \tag{17}$$
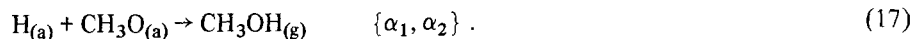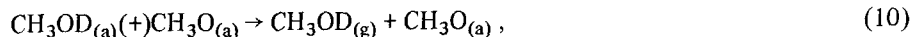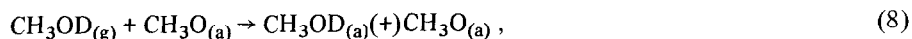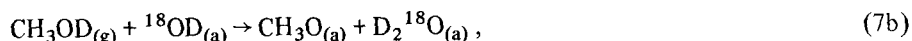
Reaction steps (11), (16), and (17) occurred primarily at 250 and 300 K, though at low coverages only the high temperature peak was observed. The H_2 peaks lagged the H_2CO peaks by about 10 K because the recombination of hydrogen atoms was not instantaneous at the temperatures and coverages used. (See Appendix I.)

The above mechanism showed that the methoxide was the *most abundant surface intermediate* during the oxidation of methanol on the Ag(110) surface, and that its surface chemistry determined the product distribution. The methoxide could (a) release a hydrogen atom to produce H_2CO (step (11)), (b) interact with

---

* The notation (+) signifies induced adsorption. Desorption steps (12) and (15) were included in the above mechanism because the desorption of these molecules from Ag(110) was not instantaneous below room temperature.

$H_2CO_{(a)}$ to form the surface complex H_2COOCH_3 at low temperatures and high coverages (step (13)), and (c) recombine with a surface hydrogen atom to form CH_3OH (step (17)). The similar behavior of the H_2CO/CH_3OD and $HCOOCH_3/CH_3OD$ peaks with CH_3OD exposure clearly indicated the importance of step (11) in the formation of $HCOOCH_3$ (see Appendix I). The chemistry of the CH_3O intermediate has been studied extensively both in the gas and liquid phases [16–22].

Various metals have been observed to stabilize alkoxide groups by forming metal alkoxides, including Be, Mg, Na, Li, La, Zr, Ti, V, Cr, Tl, Al, Th and U [17,18]. Certain alkoxide metal complexes can be oxidized to their corresponding aldehydes or ketones by removing the α-hydrogen with a base [17,18] for example,

$$\underset{R'}{\overset{R}{>}}\underset{H\ +\ :B}{\overset{O\ -\ CrO_3H}{C}} \longrightarrow \underset{R'}{\overset{R}{>}}C = O\ +\ BH^+\ +\ HCrO_3^- \tag{18}$$

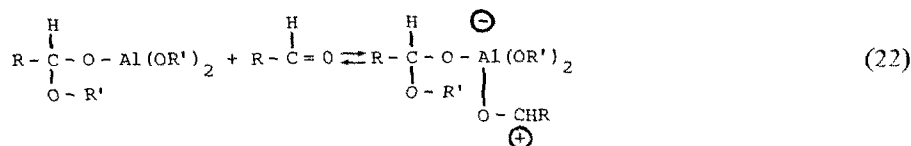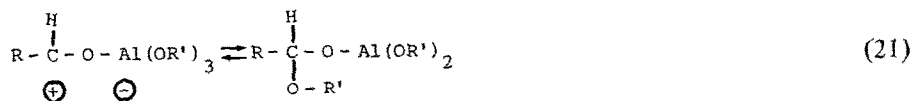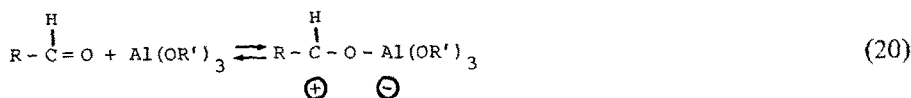This reaction is very similar to reaction step (11) which could schematically be envisioned as
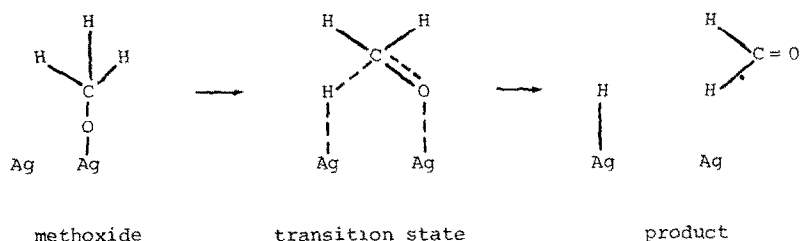
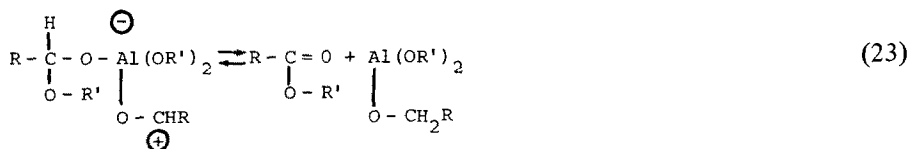where the second surface silver atom is analogous to the base of reaction (18).

The interaction of $CH_3O_{(a)}$ and $H_2CO_{(a)}$, reaction step (13), is also observed during the formation of $HCOOCH_3$ by the Tischenko reaction [20–22]

$$2\ H_2CO \xrightarrow{\ Al(OCH_3)_3\ } HCOOCH_3\ . \tag{19}$$

The alkoxide $Al(OR')_3$ has been shown to act as an alkoxide transfer agent to an aldehyde, RHCO, via the following mechanism [20–22]

$$\underset{R\ -\ C\ =\ O\ +\ Al(OR')_3}{\overset{H}{|}} \rightleftharpoons \underset{\oplus\quad\ominus}{R\ -\ \overset{H}{\underset{|}{C}}\ -\ O\ -\ Al(OR')_3} \tag{20}$$

$$\underset{\oplus\quad\ominus}{R\ -\ \overset{H}{\underset{|}{C}}\ -\ O\ -\ Al(OR')_3} \rightleftharpoons R\ -\ \overset{H}{\underset{\underset{O\ -\ R'}{|}}{C}}\ -\ O\ -\ Al(OR')_2 \tag{21}$$

$$R\ -\ \overset{H}{\underset{\underset{O\ -\ R'}{|}}{C}}\ -\ O\ -\ Al(OR')_2\ +\ R\ -\ \overset{H}{C}=O \rightleftharpoons R\ -\ \overset{H}{\underset{\underset{O\ -\ R'}{|}}{C}}\ -\ O\ -\ Al(OR')_2 \tag{22}$$

$$R - \underset{\substack{| \\ O-R' \\ | \\ \underset{\oplus}{O-CHR}}}{\overset{\overset{H}{|}}{C}} - O - Al(OR')_2 \overset{\ominus}{\rightleftharpoons} R - \underset{\substack{| \\ O-R'}}{C} = O + Al(OR')_2 \qquad (23)$$

Steps (20) and (22) involve the coordination of the aldehyde to the aluminum alkoxide. Step (21) is probably not an elementary step since the transfer of the alkoxide from the catalyst to the carbonyl carbon atom of the aldehyde is believed to involve two different aluminum alkoxides
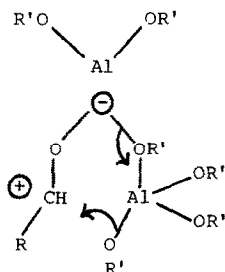
The hydride transfer step occurs in step (23) and is believed to be similar to that of Meerwein–Ponndorf reduction [17].
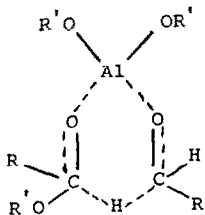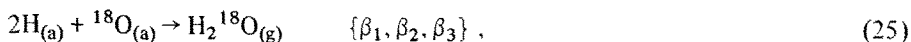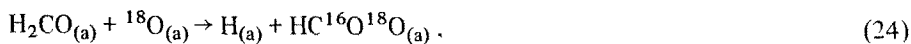
The rate-determining step in the Tischenko reaction may be either the transfer of alkoxide (step 21)) when R and R' are bulky groups because of steric interference or the hydride transfer (step (23)).

The Tischenko mechanism is the homogeneous analogue of the heterogeneous surface reaction steps (13) and (14) proposed for the attack of CH_3O on H_2CO and subsequent dissociation of the surface complex H_2COOCH_3 to $HCOOCH_3$ and hydrogen. The D_2CO and CH_3OD coadsorption studies demonstrated that hydride transfer to the Ag(110) substrate was the rate-limiting step in the formation of methyl formate. This suggested the following surface process for the production of methyl formate
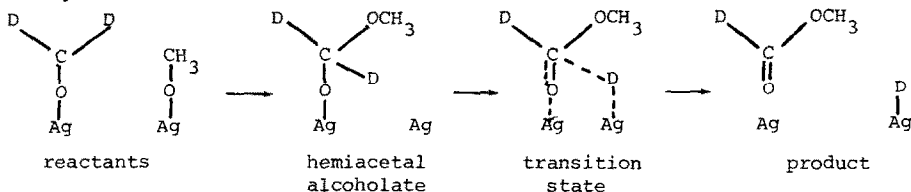
The frequency factor of $(2.4 \pm 2.0) \times 10^{11}$ sec^{-1} calculated for the above surface process appears to be a reasonable value for breaking the D–C bond through a cyclic intermediate [5]. The class of gas phase reactions similar to breaking the D–C bond of *surface intermediates* are complex fission reactions with four- or five-center cyclic transition states; frequency factors of $\sim 10^{11}$–10^{14} sec^{-1} are generally observed for gas phase fission reactions involving cyclic transition states [23]. Comparable kinetic parameters for the Tischenko reaction are not available for comparison.

The ratio of adsorbed ^{18}O to CH$_3$O determined the product distribution. Following *low* CH$_3$OD exposures to the pre-oxidized surface the ratio of surface oxygen to adsorbed methoxide was high, and the excess surface oxygen atoms further oxidized a significant amount of the formaldehyde produced. In particular, the following oxidation steps also became important *during* the flash

$$H_2CO_{(a)} + {}^{18}O_{(a)} \rightarrow H_{(a)} + HC^{16}O^{18}O_{(a)} \,. \tag{24}$$

$$2H_{(a)} + {}^{18}O_{(a)} \rightarrow H_2{}^{18}O_{(g)} \qquad \{\beta_1, \beta_2, \beta_3\} \,, \tag{25}$$

$$HC^{16}O^{18}O_{(a)} \rightarrow H_{(a)} + C^{16}O^{18}O_{(g)} \,. \tag{26}$$

$$2H_{(a)} + {}^{18}O_{(a)} \rightarrow H_2{}^{18}O_{(g)} \qquad \{\gamma\} \,, \tag{27}$$

in addition to the major reaction steps (7) to (17) presented above. As was mentioned earlier, HD^{18}O was also produced below room temperature on the unsaturated surfaces from the reaction of adsorbed ^{18}OD with surface hydrogen atoms

$$^{18}OD_{(a)} + H_{(a)} \rightarrow HD\,{}^{18}O_{(g)} \,. \tag{28}$$

H$_2$CO was directly oxidized to HC^{16}O^{18}O because the intermediate H$_2$C^{16}O^{18}O was not stable above 230 K on the Ag(110) surface [15] and the oxidation step (24) occurred at higher surface temperatures. The previous investigation [15] showed that H$_2$CO was oxidized upon adsorption on Ag(110) to H$_2$C^{16}O^{18}O which yielded HC^{16}O^{18}O at 230 K.

The C^{16}O^{18}O originated from the decomposition of the formate intermediate, HC^{16}O^{18}O, since the peak temperature was the same as that observed for the dissociation of formate from HCOOH on this Ag(110) surface [14]. Use of isotopically labeled formic acid, DCOOH, illustrated that DCOOH dissociatively adsorbed on this silver substrate at 180 K to yield the formate, DCOO, and hydrogen. The adsorbed formate intermediate was very stable and dissociated via a first-order process to simultaneously produce CO$_2$ and D$_2$ near 400 K. In the present study the C^{16}O^{18}O peak temperature was constant with coverage indicating that C^{16}O^{18}O was also produced from a first-order reaction step. The kinetic parameters for this elementary step were calculated by plotting the natural logarithm of the rate divided by the coverage against inverse surface temperature [12]. The value found was

$$k_{C^{16}O^{18}O/^{18}O,CH_3{}^{16}OD}$$

$$= (1.1 \pm 0.7) \times 10^{12} \exp(-22.2 \pm 0.5 \text{ kcal/mole} \cdot RT) \text{ sec}^{-1} \,. \tag{29}$$

This rate constant agreed well with that determined for the decomposition of formic acid on Ag(110) [14].

The *strong influence* of the oxygen to methanol ratio in determining the methanol conversions and formaldehyde yields was also observed under conventional catalytic conditions. Thomas examined the influence of the oxygen to methanol ratio upon the oxidation of methanol on silver catalysts [2]. As the weight ratio of O_2 to CH_3OH was increased from about 0.15 to 0.50, the methanol conversion rose from about 30% to about 70 to 75%; there was a drop in the formaldehyde yield from 95 to about 80%. In addition there was a simultaneous increase in conversion to CO and CO_2 (3 to 15%) and a decrease in the content of H_2 in the product gases (13 to 8%). Other investigators examined the production of formaldehyde from methanol over silver in the absence of oxygen and found low conversion [24,25] or almost no formaldehyde in the product gases [26]. The results of the present investigation are in agreement with the above observations: although oxygen is essential for the efficient production of H_2CO from methanol on silver, an excess of oxygen will further oxidize the formaldehyde to carbon dioxide and water.

The oxidation of methanol on the Cu(110) and Ag(110) catalysts exhibited many similarities, but differences were also observed. Very little methanol chemisorbed on either Cu(110) or Ag(110) in the absence of surface oxygen, and the amount of methanol adsorbed increased as a function of oxygen exposure. The enhanced activity of the partially oxidized surfaces was due to the interaction of the hydroxyl end of the CH_3OD molecule with surface ^{18}O atoms during the adsorption process to form adsorbed CH_3O and $D_2{}^{18}O$. $D_2{}^{18}O$ was thus selectively formed on both surfaces. During adsorption of CH_3OD at 180 K, $D_2{}^{18}O$ was displaced from the Ag(110) surface into the gas phase, but similar displacement from the Cu(110) surface did not occur. This weaker binding observed for CH_3OD on Ag(110) generally reflects the weaker adsorbate–substrate bonds exhibited by the Ag(110) surfaces. This observation included the desorption of O_2 which desorbed from the Ag(110) substrate, but not from the Cu(110) substrate at comparable surface coverages. Adsorbate–substrate bonds evidently were stronger on copper than on silver.

With regard to the reaction mechanism for methanol oxidation on Cu(110) and Ag(110), the reaction steps were very similar but the Ag(110) surface was more active for the decomposition of the surface intermediates. Both reactions proceeded via methoxide and formate intermediates, and methoxide was the most abundant surface intermediate on both substrates. The methoxide exhibited the same surface chemistry, with the exception of steps (13) and (14), on the Ag(110) and Cu(110) surfaces. Although Cu(110) and Ag(110) displayed similar reaction mechanism, the different activities of the two surfaces resulted in different selectivities.

The selectivity on the Cu(110) catalyst was determined by the *intermediates formed upon adsorption* but on the Ag(110) catalyst the selectivity was also determined by *reactions taking place during the flash*. Methyl formate was formed on Ag(110) from the interaction of CH_3O and H_2CO, but methyl formate was not

observed on Cu(110). This interaction occurred on Ag(110) and not on Cu(110) because silver was much more active for the decomposition of $CH_3O_{(a)}$ to H_2CO, and formaldehyde was thus produced at much lower substrate temperatures which resulted in longer surface residence times for H_2CO on Ag(110). Although H_2CO/H_2CO desorbed at the same surface temperatures from Cu(110) and Ag(110), the surface residence time of formaldehyde was estimated to be longer by a factor of $\sim 5 \times 10^3$ at 250 K than at 365 K. Thus the selectivity was strongly dependent on the extent adsorbed CH_3O and H_2CO interacted on the surface. Methyl formate was not observed as a reaction product in the industrial oxidation of methanol over silver catalysts [1] because the commercial process operates at much higher temperatures, about 600°C, and the surface residence time of formaldehyde is extremely small. The reaction selectivity was also dependent on the extent to which the reaction products were further oxidized. There was no evidence on the Cu(110) surface that H_2CO/CH_3OD was further oxidized when excess surface oxygen was present because the $C^{16}O^{18}O$ signal *did not decrease* with increasing methanol exposures, as was observed on the Ag(110) catalyst. The much weaker adsorbate—substrate bond for oxygen on the silver substrate was probably responsible for the larger significance of the oxidation reactions on Ag(110) at low methanol coverages (step (24) to (28)). Since the oxygen atom was held more tightly by the copper substrate, it was probably more difficult to reduce the partially oxidized copper surface, resulting in the lesser importance of oxidation of H_2CO on copper during the flash. Silver and copper catalysts display very similar characteristics during the commercial oxidation of methanol because excess methanol is employed and the reaction temperatures are high [1].

5. Conclusions

The results of this study clearly indicated that surface oxygen atoms created the active sites for the oxidation of methanol to formaldehyde and that methanol dissociatively chemisorbed on the Ag(110) surface as CH_3O. Methoxide was observed to (a) decompose to formaldehyde and hydrogen, (b) recombine with a surface hydrogen atom to yield methanol, and (c) interact with surface formaldehyde to form a hemiacetal alcoholate which subsequently decomposed to methyl formate and hydrogen. Furthermore, in the presence of excess surface oxygen formaldehyde was oxidized to HCOO. Methoxide was the most abundant surface intermediate, and its surface chemistry and the ratio of surface oxygen to methoxide determined the final product distribution.

The oxidation of methanol on Cu(110) and Ag(110) exhibited many similarities, but differences were also observed. The reaction mechanisms were essentially the same on both catalyst surfaces with the exception of the absence of hemiacetal alcoholate on Cu(110). The rate constants for the different surface reactions were substantially higher on the Ag(110) surface, and the Cu(110) surface exhibited

stronger adsorbate—substrate bonds. In reactions operating in the flow mode the relative overall rates for the oxidation of methanol on copper and silver catalysts may be different because the relative rates for the dissociative adsorption of oxygen and methanol must also be considered. This may become important if the slow step of the process is the dissociative adsorption of oxygen on the catalyst surface because the sticking probability of oxygen was found to be approximately an order of magnitude lower on Ag(110) than on Cu(110).

Acknowledgement

Note added

HCO was apparently not involved as a stable intermediate in the production of $HCOOCH_3$, since the Ag surface did not dissociately adsorb H_2CO to form H_2 or CO and no CO was observed following coadsorption of D_2CO and CH_3OD. The necessary conclusion was that $D_2CO_{(a)}$ and $CH_3O_{(a)}$ formed a strongly coupled system which is denoted as D_2COOCH_3.

Appendix I. The effects of CH_3OD exposure on the kinetics of formation of CH_3OD, H_2, H_2CO and CH_3OH from CH_3OD

The data presented in this Appendix are included to support and expand upon the arguments presented in the text. As will be shown below, these data indicated that (1) CH_3OD desorption was first-order with an accompanying decrease in binding energy of 1—4 kcal/gmol with increasing coverage, (2) CH_3OH was reversibly formed from $CH_3O_{(a)}$, and (3) the CH_3OH, H_2CO and $HCOOCH_3$ product peaks evolved in nearly identical fashion as the exposure to CH_3OD was increased. The products are considered in turn below.

CH_3OD/CH_3OD

The flash desorption spectra of CH_3OD are presented in fig. 9 as a function of exposure; the Ag(110) surface was preoxidized at 295 ± 10 K and methanol was adsorbed at 180 K. At low coverages two CH_3OD binding states were present as shown in curve (a) like those for $D_2{}^{18}O$, and the desorption peaks shifted to lower temperatures with increasing coverage. This shift could have been due to a nonlinear desorption kinetics of CH_3OD (i.e. if CH_3OD were formed from the recom-

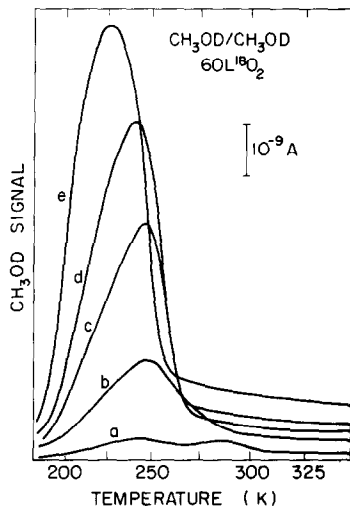Fig. 9. The CH₃OD desorption spectra subsequent to the adsorption of CH₃OD at 180 K on a Ag(110) surface predosed with $^{18}O_2$ at 295 ± 10 K. 60 L of oxygen was applied with the M.S. on. The CH₃OD exposures were (a) 5 sec, (b) 13 sec, (c) 19 sec, (d) 25 sec and (e) 75 sec.

bination of $CH_3O_{(a)}$ and $D_{(a)}$) or a weakening of the CH_3OD substrate bond with increasing coverage on the Ag(110) surface. The recombination reaction would require the presence of deuterium atoms on the surface and thus some D_2 or HD should have been detected. Since neither D_2 nor HD were observed during the flash, the decrease in the CH_3OD peak temperature was not due to a second-order reaction to form CH_3OD, but to a coverage dependent CH_3OD substrate binding energy. If the frequency factor for the desorption of CH_3OD was assumed to be 10^{13} sec^{-1} the CH_3OD binding states were weakened by 1–4 kcal/mole with increasing coverage.

H_2/CH_3OD

The H_2 desorption spectrum following a high CH_3OD exposure was presented in fig. 3 and essentially the same spectrum, both in magnitude and peak positions, was observed at all methanol exposures. Although the major H_2/CH_3OD peaks corresponded to the H_2CO/CH_3OD peaks, hydrogen was produced on the Ag(110) surface from several reaction pathways that depended on the concentration of oxygen atoms present on the surface during the flash. Subsequent to high exposures of methanol, hydrogen was released when the surface intermediates H_2COOCH_3 and CH_3O dissociated to $HCOOCH_3$ and H_2CO, respectively; subsequent to low exposures of methanol hydrogen was also released when H_2CO was oxidized to formate and again when the formate decomposed to carbon dioxide. Hydrogen also reacted

with other surface intermediates, and the particular reaction pathway for the removal of surface hydrogen was related to the presence of excess oxygen atoms on the Ag(110) surface subsequent to the adsorption of methanol. Following high exposures of methanol the surface hydrogen atoms recombined with methoxide to yield CH_3OH; following low exposures of methanol hydrogen was also oxidized to $H_2^{18}O$. The various reaction paths supplying and removing hydrogen atoms from the surface apparently maintained the magnitude of the H_2/CH_3OD signal relatively constant over the range of methanol exposures examined.

CH_3OH/CH_3OD

The CH_3OH temperature programmed spectra subsequent to the adsorption of CH_3OD at 180 K on the Ag(110) surface that was preoxidized with $^{18}O_2$ at 295 ± 10 K is presented in fig. 10 as a function of methanol exposure. The CH_3OH spectra was recorded by monitoring the $m/e = 31$ signal which also contained substantial contributions from cracking of $HCOOCH_3$ at 250 and 280 ± 3 K (see Appendix II). More than half of the $m/e = 31$ signal was due to CH_3OH. The fragmentation of $HCOOCH_3$ in the mass spectrometer did not alter the peak positions of the $CH_3OH(\alpha_1)/CH_3OD$ and $CH_3OH(\alpha_2)/CH_3OD$ signals, since they also appeared at the same temperature (252 and 280 ± 3 K), but they did increase the magnitude of the $m/e = 31$ signals in fig. 10. The simultaneous formation of CH_3OH and $HCOOCH_3$ at 250 ± 2 and 280 ± 3 K revealed that the intermediate $CH_3O_{(a)}$ reacted with the surface hydrogen atoms released by the formation of $HCOOCH_3$ from H_2COOCH_3, reaction step (3), to form CH_3OH. Two additional and much smaller CH_3OH/CH_3OD peaks, β_2 and β_3, were also present at about 300 and 340
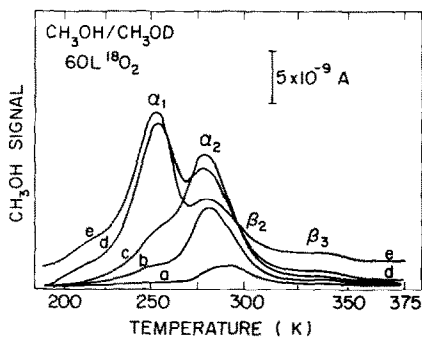

Fig. 10. The CH_3OH desorption spectra obtained by monitoring $m/e = 31$ subsequent to the adsorption of CH_3OD at 180 K on a partially oxidized Ag(110) surface. The surface was pre-dosed with 60 L $^{18}O_2$ at 295 ± 10 K while the M.S. was on. These CH_3OH spectra were *not corrected* for substantial cracking contributions of $HCOOCH_3$. The CH_3OD exposures were (a) 5 sec, (b) 13 sec, (c) 25 sec, (d) 50 sec and (e) 75 sec.
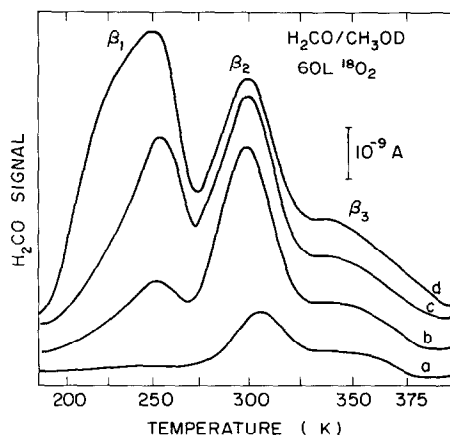
Fig. 11. The H_2CO temperature programmed spectra as a function of CH_3OD exposure. The Ag(110) surface was always predosed by 60 L $^{18}O_2$ with the M.S. on at 295 ± 10 K prior to the adsorption of CH_3OD at 180 K. The CH_3OD exposures were (a) 5 sec, (b) 13 sec, (c) 25 sec and (d) 75 sec.

K. The β_2 peak is not well defined in fig. 10 because it is smaller than the α_2 peak, but its presence was verified when the sensitivity of the CH_3OH signal was increased. These additional peaks were not related to the formation of methyl formate, since methyl formate peaks were not present in this temperature range (see fig. 5). These additional CH_3OH/CH_3OD peaks corresponded to those observed for H_2CO/CH_3OD and H_2/CH_3OD and will be further discussed below in conjunction with formaldehyde production.

H_2CO/CH_3OD

The H_2CO/CH_3OD spectra from the partially oxidized Ag(110) surface are shown in fig. 11 as a function of CH_3OD exposure at 180 K. Several pathways for the formation of H_2CO from CH_3OD were evident as indicated by the β_1, β_2 and β_3 peaks. The invariance of the H_2CO/CH_3OD β_1, β_2 and β_3 peak temperatures with coverage demonstrated that the production of H_2CO occurred via first-order processes on this Ag(110) surface. The evolution of formaldehyde from this surface at 250 K and above was not desorption-limited and represented reaction-limited step since H_2CO/H_2CO desorbed from Ag(110) near 228 K (see table 2). The kinetic parameters for the formation of H_2CO from CH_3OD could not be accurately determined because of the overlap of the different H_2CO peaks. The simultaneous production of H_2CO/CH_3OD and CH_3OH/CH_3OD at approximately 250, 300 and 340 K revealed that both products originated from the same surface intermediate, CH_3O. It was concluded from these observations that formaldehyde was produced from the decomposition of the surface methoxide.

Table 5
The mass spectrum of HCOOCH$_3$

m/e	Abundance
31	100
29	70
32	40
15	30
60	22
28	22
30	7
44	3

Appendix II. Product identification by mass spectrometry

The various signals that desorbed from the partially oxidized Ag(110) surface following adsorption of CH$_3$OD were readily identified by mass spectrometry. The major ionization peaks of HCOOCH$_3$ (M = 60) are presented in table 5 and were obtained in the present study; this spectrum was the same as that reported by other investigators [27]. The HCOOCH$_3$ molecule gave rise to large m/e = 31, 32, 29 and 60 signals; the m/e = 60 signal was used to monitor HCOOCH$_3$ and is shown in fig. 12 following the adsorption of CH$_3$OD on the partially oxidized silver surface. Methyl formate was distinguished from glycol aldehyde,
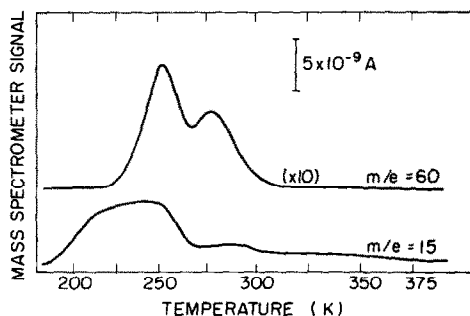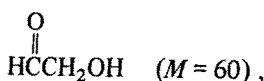
$$\overset{\displaystyle O}{\overset{\|}{H}C}CH_2OH \quad (M = 60) ,$$

Fig. 12. The m/e = 60 and 15 signals subsequent to the adsorption of CH$_3$OD at 180 K on a Ag(110) surface that was predosed with $^{18}O_2$ at 295 ± 10 K.

Table 6
The mass spectrum of CH_3OH and CH_3OD (from Beynon, Fontaine and Lester [28])

m/e	CH_3OH		m/e	CH_3OD	
	Identity	Abundance		Identity	Abundance
31	CH_2OH	100	32	CH_2OD	100
32	CH_3OH	80	33	CH_3OD	79
29	CHO	33	29	CHO	18
15	CH_3	10	15	CH_3	10

which also gives rise to substantial $m/e = 31$, 32, 29 and 60 signals [27] by the small $m/e = 44$ (CO_2^-) signal present *only* in the $HCOOCH_3$ spectrum.

The major ionization peaks of CH_3OH ($M = 32$) and CH_3OD ($M = 33$) in the mass spectrometer are presented in table 6 [28]. The CH_3OH molecule gives rise to large $m/e = 31$, 32, 29 and 15 signals and the CH_3OD molecule gives rise to large $m/e = 32$, 33, 29 and 15 signals. The two forms of methanol are thus distinguishable by monitoring $m/e = 33$ for CH_3OD and $m/e = 31$ for CH_3OH. The $m/e = 33$, 32 and 31 signals were recorded subsequent to the adsorption of CH_3OD on a partially oxidized Ag(110) surface and are shown in fig. 13. Only $m/e = 33$ and 32 signals appeared near 225 K and they originated from CH_3OD; only $m/e = 32$ and 31 signals appeared at 250 K and at higher temperatures and they originated from CH_3OH and cracking contributions of $HCOOCH_3$. The $m/e = 31$ spectrum was representative of the CH_3OH signal, as discussed below. The $m/e = 15$ signal was also monitored and presented in fig. 12; the signal is a composite of the CH_3OH and CH_3OD spectra since both molecules give rise to CH_3^+ signals. Thus CH_3OH was
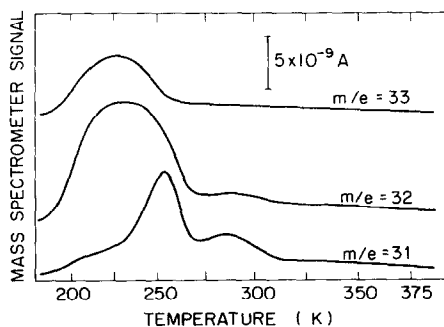

Fig. 13. The $m/e = 33$, 32 and 31 signals subsequent to the adsorption of CH_3OD at 180 K on a Ag(110) surface that was predosed with $^{18}O_2$ at 295 ± 10 K.
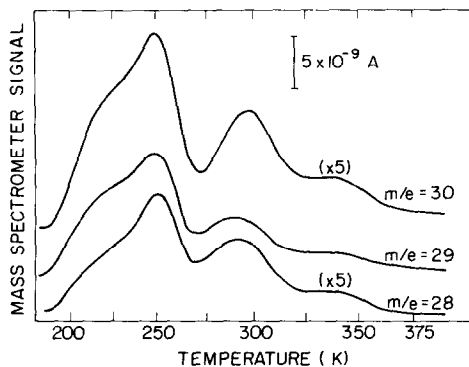
Fig. 14. The m/e = 30, 29 and 28 signals subsequent to the adsorption of CH_3OD at 180 K on a Ag(110) surface that was predosed with $^{18}O_2$ at 295 ± 10 K.

monitored by recording the m/e = 31 signal and CH_3OD was recorded by monitoring the m/e = 33 signal.

More than half of the m/e = 31 signal could not be accounted for by the contribution of $HCOOCH_3$ and was thus attributed to CH_3OH. This is readily evident when the $HCOOCH_3/CH_3OD$ and the CH_3OH/CH_3OD spectra are compared subsequent to a 25 sec exposure of CH_3OD; curve (d) of fig. 5 and curve (c) of fig. 10, respectively. The $HCOOCH_3$ spectrum shows approximately equal amounts of methyl formate desorbing from the α_1 and α_2 peaks, but the CH_3OH spectrum does not show a prominant α_1 peak. Thus CH_3OH was a reaction product from the oxidation of CH_3OD on Ag(110) whose α_1 and α_2 peak temperatures were indistinguishable from $HCOOCH_3/CH_3OD$. Since more than half of the m/e = 31 signal arose from CH_3OH and appeared to retain the CH_3OH characteristics, the CH_3OH/CH_3OD spectra presented in fig. 10 were not corrected for the $HCOOCH_3$ contributions.

Formaldehyde, H_2CO (M = 30), that resulted from the oxidation of methanol on Ag(110) was monitored by recording the m/e = 30 signal because neither CH_3OH, CH_3OD nor $HCOOCH_3$ gave rise to substantial m/e = 30 signals. The cracking pattern of H_2CO contains significant m/e = 29, 30 and 28 signals [29]. The m/e = 30, 29 and 28 signals were recorded subsequent to the adsorption of CH_3OD on a partially oxidized Ag(110) surface and are shown in fig. 14. This spectrum in conjunction with the coverage variation results verified that H_2CO was a major reaction product from the oxidation of methanol on Ag(110).

The various isotopes of water were monitored by recording the m/e = 22 ($D_2{}^{18}O$), the m/e = 21 (HD ^{18}O), and the m/e = 20 ($H_2{}^{18}O$) signals. The $H_2{}^{18}O$ signal was corrected for $^{18}OD^+$ contributions from $D_2{}^{18}O$ and HD ^{18}O [29]. The isotopes of carbon dioxide did not give rise to overlapping signals and were identified by recording the m/e = 48 ($C^{18}O^{18}O$), m/e = 46 ($C^{16}O^{18}O$), and m/e = 44 ($C^{16}O^{16}O$) signals.

References

[1] J.F. Walker, Formaldehyde (Reinhold, New York, 1964) pp. 1−36.

[2] M.D. Thomas, J. Am. Chem. Soc. 42 (1920) 867.

[3] C.L. Thomas, Catalytic Processes and Proven Catalysts (Academic Press, New York, 1970) p. 208.

[4] J.K. Dixon and J.E. Longfield, in: Catalysis, Vol. 7, Ed. P.H. Emmet (Reinhold, New York, 1960) pp. 231−236.

[5] I.E. Wachs and R.J. Madix, submitted J. Catalysis.

[6] J. McCarty, J. Falconer and R.J. Madix, J. Catalysis 30 (1973) 235.

[7] A.M. Bradshaw, A. Engelhardt and D. Menzel, Ber. Bunsenges. Physik. Chem. 76 (1972) 500;
H.A. Engelhardt and D. Menzel, Surface Sci. 57 (1976) 591.

[8] G. Rovida and F. Pratesi, Surface Sci. 52 (1975) 542.

[9] L.E. Davis, N.C. McDonald, P.W. Palmberg, G.E. Riach and R.E. Weber, Handbook of Auger Electron Spectroscopy (Physical Electronics Industries, Minnesota, 1976) p. 131.

[10] W.A. Coglan and R.E. Clausing, A. Catalog of Calculated Auger Transitions for the Elements (National Technical Information Service, ORNL-TM-3576, November 1971, pp. 149−153.

[11] S. Miller and R.J. Madix, unpublished results.

[12] J. Falconer and R.J. Madix, Surface Sci. 48 (1975) 393.
J. Falconer and R.J. Madix, J. Catalysis 48 (1977) 262.

[13] R.T. Morrison and R.N. Boyd, Organic Chemistry (Allyn and Bacon, Boston, 1966) p. 602.

[14] S. Miller and R.J. Madix, to be published.

[15] I.E. Wachs and R.J. Madix, unpublished results.

[16] J. Heicklen, in: Oxidation of Organic Compounds, VII, Proc. Intern. Oxidation Symp., San Francisco, 1967 (American Chemical Society, Washington, DC, 1968) pp. 31−38.

[17] R. Stewart, Oxidation Mechanisms: Applications to Organic Chemistry (Benjamin, New York, 1964) pp. 35−40.

[18] J. March, Advanced Organic Chemistry (McGraw-Hill, New York, 1977) pp. 1082−1084.

[19] D.C. Bradley, Progr. Inorgan. Chem. 2 (1960) 303.

[20] Y. Ogata, A. Kawasaki and I. Kishi, Tetrahedron 23 (1967) 825.

[21] Y. Ogata and A. Kawasaki, Tetrahedron 25 (1969) 929.

[22] T. Saegusa, T. Ueshima and S. Kitagawa, Bull. Chem. Soc. Japan 42 (1969) 248.

[23] S.W. Benson, Thermochemical Kinetics (Wiley, New York, 1968) pp. 75−82.

[24] I.P. Planovskaya and K.V. Topchieva, Kinetik i Kataliz 2 (1961) 375.

[25] V.I. Atroshchenko and I.P. Kushnarenko, Intern. Chem. Eng. 4 (1964) 581.

[26] S.K. Bhattacharyya, N.K. Nag and N.D. Ganguly, J. Catalysis 23 (1971) 158.

[27] S.D. Worley and J.T. Yates, J. Catalysis 48 (1977) 395.

[28] J.H. Beynon, A.E. Fontaine and G.R. Lester, J. Mass Spectr. Ion Phys. 1 (1968) 1.

[29] E. Stenhagen, S. Abrahamson and F.W. McLafferty, Eds., Atlas of Mass Spectral Data, Vol. 1 (Interscience, New York, 1969).